trol valve
p_i = actuating pressure of cooling water control valve
q_C = output of controller
q_h = material flow rate to heat exchanger
q_i = inflow rate of material to be cooled
q_S = output of temperature sensor
q_V = flow rate of cooling water
S = internal mode of temperature sensor
T_i = temperature of material into heat exchanger
T_o = temperature of material out of heat exchanger
V_2 = internal mode of cutoff valve
V_5 = internal mode of cooling water control valve

LITERATURE CITED

Fussell, J. B., and W. E. Vesely, "A New Methodology for Obtaining Cut Sets for Fault Trees," *Trans. Am. Nucl. Soc.*, **15**, 262 (1972).

Fussell, J. B., "Synthetic Tree Model—A Formal Methodology for Fault Tree Construction," *ANCR-1098*, Available from NTIS, Springfield, Va. (1973).

———, "Fault Tree Analysis—Concepts and Techniques," in *Generic Techniques of System Reliability Assessment*, E. Henley and J. Lynn, ed., Nordhoff Publishing Company (1976).

Henley, E. J., and H. Kumamoto, "Comments on Computer-Aided Synthesis of Fault Trees," *IEEE Trans. Reliability*, **R-26** (1977).

Lapp, S. A., and G. J. Powers, "Computer-Aided Synthesis of Fault-Trees," *ibid.*, (1977).

Pollack, S. L. *Decision Tables: Theory and Practice*, Wiley-Interscience, New York (1971).

Salem, S. L., G. E. Apostolakis, and D. Okrent, "A New Methodology for the Computer-aided Construction of Fault Trees," *Ann. Nucl. Energy*, **4**, 433 (1977).

Vesely, W. E., and R. E. Narum, "PREP and KITT; Computer Codes for the Automatic Evaluation of a Fault Tree," IN-1349, Available from NTIS, Springfield, Va. (1970).

Manuscript received January 13, 1978; revision received August 7, and accepted August 25, 1978.

Mass Transfer in Regular Arrays of Hollow Fibers in Countercurrent Dialysis

ISAO NODA

and

CARL C. GRYTE

Department of Chemical Engineering and Applied Chemistry
Columbia University
New York, New York 10027

The concentration profiles in a countercurrent hollow fiber bundle mass exchanger dialyzer is derived, assuming a uniform distribution of fibers in the dialyzer shell. Mass transfer coefficients are obtained as a function of fiber packing density, membrane thickness, membrane material, and solute type.

SCOPE

Dialysis is a membrane separation process which involves diffusive transport of a solute from one fluid to another. Although the solute flux is often accompanied by some volumetric flux across the membrane, driven either by hydraulic or osmotic pressure, we shall focus here only on diffusive transport systems. The input-output response of a continuous dialysis unit using various flow geometries is given by Michaels (1966). The rate of mass transfer of a solute across the membrane during dialysis is expressed in terms of the surface area, the concentration difference across the membrane, and the overall mass transfer coefficient. The magnitude of the overall mass transfer coefficient for a given dialyzer is usually determined experimentally. Dialysis membranes in the form of hollow fibers are gaining considerable attention because, in this configuration, large membrane surface areas are obtained for a given dialyzer volume. The most significant application is in the area of hemodialysis (Klein et al., 1976*a*). Recently, Noda (1976) has proposed highly selective multistaged dialysis separation processes.

Much data are available for the individual polymeric membrane materials (Colton, 1971; Klein et al., 1977). Detailed theoretical descriptions are reported to account for dialysis with planar membrane surfaces (Leonard, 1968), but only simplistic models are available to describe the mass transfer in closely packed hollow fiber bundles. Stevenson (1975) has reported a method for determining the membrane permeability of a single, isolated, hollow fiber. Methods have been proposed by Klein et al. (1977) to characterize bundles of well-separated hollow fibers empirically. A discussion of the problems associated with the characterization of a hollow fiber bundle similar to that used in hemodialysis has been recently given by Klein et al. (1976*a*, 1976*b*). In all studies, however, the procedure has been to reduce the analysis to that of a single isolated fiber [equivalent annulus approximation, Happel (1959)], thereby neglecting the interactions between fibers which become important when the interfiber distances are small.

The aim of this investigation is to establish a theoretical understanding of hollow fiber dialysis systems by using a

simple distribution model of fibers in a dialyzer shell. The mass transfer coefficients are calculated for the case of countercurrent equal volumetric flow. The effects of packing density, membrane thickness, and properties of membrane material and solute on the overall mass transfer coefficient of a hollow fiber dialyzer are studied.

CONCLUSIONS AND SIGNIFICANCE

The concentration profile in a countercurrent hollow fiber dialyzer bundle is derived from the differential mass balances for a solute inside the hollow fiber, in the fiber membrane, and in the extra fiber space. The overall mass transfer coefficient, calculated from the concentration profile, is found to be a function of the packing density of the hollow fibers in the dialyzer shell as well as the thickness of the fiber membrane, the type of membrane, and the nature of the solute. Efficient mass transfer in a hollow fiber dialyzer cannot always be obtained simply by packing the fibers tightly in the dialyzer shell, since the calculated results for the mass transfer coefficients indicate that there is an optimal packing density of the fibers. Very tightly packed hollow fiber dialyzers actually suffer from a decrease in available membrane surface area and are expected to have a lower efficiency. The effect of packing density becomes important if the membrane is very thin or very permeable to the solute.

Correlation curves to calculate the estimated value of the mass transfer coefficient of a hollow fiber dialyzer from the known value of the membrane permeability are supplied. This correlation is useful because even though experimental data of membrane permeability are often found in the literature, the computation of the input-output response of a hollow fiber dialyzer requires knowledge of the overall mass transfer coefficient. The present result, obtained without neglecting the effects of the interactions between neighboring fibers, is one of the few detailed descriptions of the mass transfer characteristics of such systems.

The geometric structure of hollow fiber dialyzers resembles that of classical shell and tube heat exchangers. There are, however, several important differences between the two systems. Unlike the heat exchangers, the length-to-diameter ratio of a typical channel in a well-packed hollow fiber dialyzer often has a value as large as 10^3 to 10^4. The entry region effect, which is important in ordinary heat exchangers, becomes practically negligible for this sort of unit. The transfer resistance of dialyzers is more or less localized in the membrane phase which is usually less permeable for a given solute than the free solution phase. The Reynolds number for a well-packed hollow fiber dialyzer is very low; that is, the dialysis is carried out with laminar flow. These peculiarities of a hollow fiber dialyzer somewhat restrict the direct application of heat exchanger data for mass transfer characterization.

The development of transfer characteristics in a convective-diffusive mass transfer problem usually requires knowledge of the flow pattern of the fluid in the system. The two streams of solution in a dialyzer, one flowing through the inside of the numerous hollow fibers and the other through the extra fiber space in the fiber bundle, have quite different velocity profiles. The velocity profile of the flow inside the fibers has a simple parabolic shape

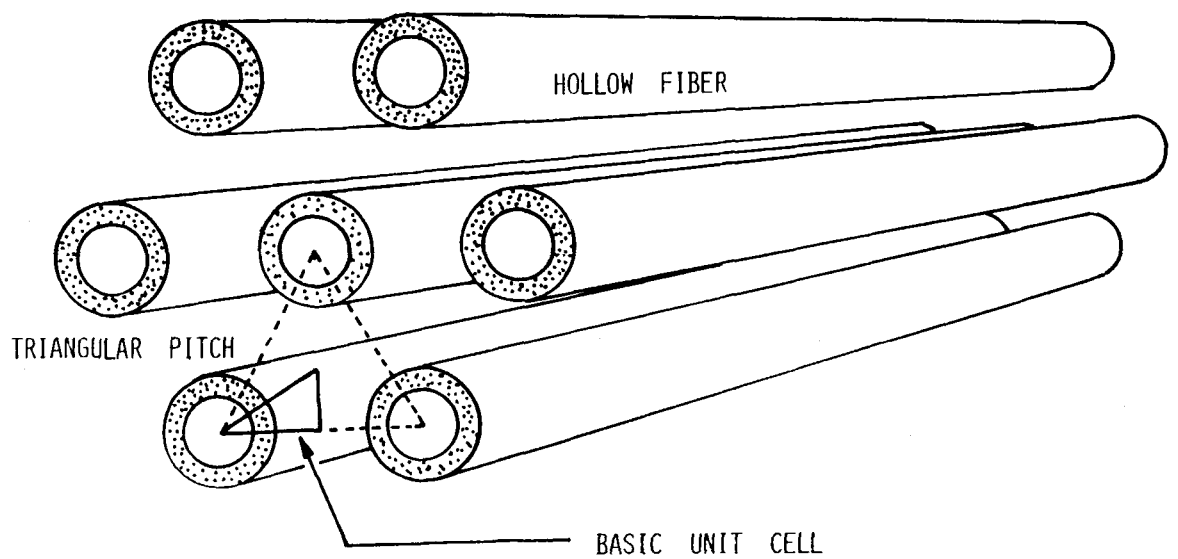

Fig. 1. Regular array of hollow fibers. Triangular pitch.

of Poiseuille flow, but the flow outside of the fibers has a much more complicated velocity profile. The outside velocity profile, controlled by the geometric distribution of individual fibers in the dialyzer shell, in turn, will strongly influence the cross-sectional concentration profile of a solute not only outside the fiber but within the fiber as well.

The convective heat transfer problem for parabolic flow in a circular duct with a uniform temperature and heat flux at the periphery has been studied by many investigators (Graetz, 1885; Drew, 1931; Sellars, 1956). Their results are not directly applicable to our system without modification, since the concentration and flux at the periphery of a hollow fiber are expected to be irregular owing to the interaction between fibers. The study of the convective mass transfer problem, even for the flow inside a hollow fiber, is severely limited by the extent of the present understanding of the behavior of a fluid flowing through the interfiber space of the fiber bundle in the dialyzer shell.

Experimental studies of flow through compact bundles of circular fibers have been conducted by Sullivan (1942). Although the random packing of the fibers used by Sullivan resembles closely the configuration of hollow fibers in a dialyzer shell, the analytic, development of the concentration profiles, of a random system is extremely difficult and not suited to our purpose. One of the earliest attempts to analyze a flow in a uniform array of rod bundles with a very large spacing is given by Emersleben (1925). The equivalent annulus, or free surface model (Happel, 1959), which assumes a cylindrical flow envelope surrounding each rod, has been very successful in describing the flow through a bundle of rods when the spacing between rods is relatively large. Sparrow and Loeffler (1959) studied a model which describes the flow through a regular array of cylindrical rods. They derived the solution for the velocity profile of a flow through an infinite and regular array of cylindrical rods arranged either in an equilateral triangular pitch or in a square pitch for a well-developed laminar flow. The flow pattern and the friction factor are strongly dependent on the spacing between the rods. Axford (1967) and Dwyer (1970) have recalculated the series constants of the Sparrow-Loeffler solution for the case when the rods are very tightly packed. Shih (1967) proposed a modified mathematical procedure for the Sparrow-Loeffler problem. The effects of a wall around a bundle of uniformly spaced fibers on the flow have been considered by Schmid (1966), who has reported that the effect of the wall does not penetrate into the rod bundle farther than the first row of rods adjacent to the wall if the spacing between the rods is not very large. Further investigations of the effects of the surrounding shell have been carried out by other authors both for turbulent flow (Rheme, 1972) and laminar flow (Mottaghin, 1972). Experimental results for the flow through a regular array are given by Presser (1971).

Although the shell and tube heat exchangers have been used for many years, the development of theoretical analysis for the laminar convective heat transfer problem using the velocity profile obtained for flow through a regular array of rods is found mainly in the field of nuclear reactor design. Sparrow (1961) considered the heat transfer problem for rods arranged in a triangular pitch, assuming constant axial heat transfer and a uniform peripheral temperature. A similar problem with uniform peripheral heat flux is solved by Dwyer (1970), and the existence of an optimal spacing between the rods for heat transfer is mentioned. The results are compared with those of Sparrow (1961). Axford (1967) solved a multiregion problem with a similar array of rods. He assumed a uniform volumetric generation of heat within the fuel rods. The temperature profiles are solved for the coolant, the cladding, and the fuel regions simultaneously, using a Fourier cosine transform. The peripheral heat flux and the temperature are found to be nonuniform for his boundary conditions.

The direct application of the Sparrow-Loeffler solution is rarely seen in the study of convective mass transfer problems, although the equivalent annulus model and the truncated form of the Sparrow-Loeffler solution have been used. Hollow fiber reverse osmosis, not dialysis, has been studied by Gill (1973), using the equivalent annulus model; a much more simplified treatment is given by Doshi (1977). Winograd (1971, 1974) used the truncated Sparrow-Loeffler solution to study shell and tube countercurrent systems for ion exchange and reverse osmosis units. The application of the equivalent annulus model in mass transfer is also mentioned by Waterland (1974) and, in a more refined manner, by Kim and Cooney (1976). Their analysis of hollow fiber mass transfer is limited to the condition in which the extra fiber space containing immobilized enzymes is quiescent. A capillary bed in biological systems, first described by Krough (1918), is analogous to the enzyme hollow fiber system in which no bulk flow occurs in the extra fiber space. Further discussion on heat and mass transfer in biological systems is given by Lih (1975). Recently, Frankel and Wei (1977) have reported detailed model calculations of an artificial capillary bed system in which the extra capillary space is perfused by ultrafiltration from one set of hollow fibers to another.

ANALYSIS

Uniform Fiber Distribution Model

In an ordinary dialyzer, numerous hollow fibers are packed randomly in a long shell, and the exact distribution of the fibers in a shell is rarely known. The irregular configuration of fibers caused by the random packing makes it very difficult, if not impossible, to develop a simple mathematical representation of the concentration profiles in the dialyzer. In order to overcome this difficulty, we have introduced a simple model (Figure 1) such that the individual fibers are packed in an infinite regular array. The choice of the equilateral triangular array is rather arbitrary; other regular configurations such as a square array can be selected with only minor changes in the boundary conditions. The effect of the shell wall surrounding the bundle of hollow fibers is neglected, since the number of fibers used in a dialyzer of this kind is usually very large.

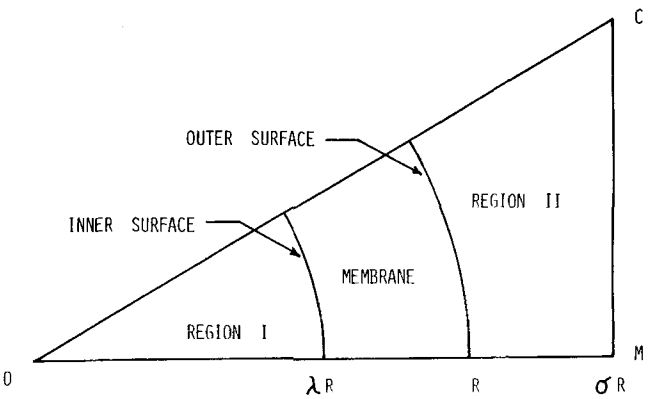

Fig. 2. Basic unit cell of the array of hollow fibers. The angle MOC is π/6.

From the symmetric properties of the regular array, it is evident that only the basic unit cell (Figure 2) must be considered. The entire cross section of a dialyzer is composed of a regular array of such cells. The unit cell is divided into three different regions: the region inside the hollow fiber (I); the membrane (M); and the region outside the fiber (II). The dimensions of the unit cell are given by the outer radius R, the inner radius λR, and the distance $\overline{OM}$ which is one half of the distance between two adjacent fibers. This fiber-to-fiber distance is called the pitch of the array. By selecting the outer radius R as a characteristic length of the unit cell, two dimensionless geometric parameters are defined: the inner-to-outer diameter ratio λ and the pitch-to-diameter ratio σ. One other dimensionless number which is a function of the solute type and the membrane material is defined. The effective membrane diffusivity $\mathcal{D}^M_{\text{eff}}$ (Colton, 1971) of the solute is given by:

$$\mathcal{D}^M_{\text{eff}} = K\mathcal{D}^M \tag{1}$$

For the present development, K is considered identical on the inside and outside surfaces of the membrane. The effective membrane diffusivity-to-free solution diffusivity ratio ξ is defined as

$$\xi = \mathcal{D}^M_{\text{eff}}/\mathcal{D} \tag{2}$$

In addition to the uniform distribution of the fibers, several simplifying assumptions are made: the physical constants, such as the fluid viscosity μ and the diffusivity of the solute $\mathcal{D}$, have the same value both in region I and II; the fiber membrane is isotropic; and the volumetric flux of the fluid across the membrane, driven either by hydraulic or osmotic pressure, is very small. The analysis will be focused on the well developed concentration profile case. For a dialyzer made of hollow fibers whose length-to-diameter ratio is very large, the entry region effect is negligible.

Velocity Profiles

The fluid velocity v^I for the flow through the inside of a hollow fiber, region I, is expressed by that of parabolic Poiseuille flow

$$v^I = -\frac{dP^I}{dz}\left(\frac{\lambda^2R^2}{4\mu}\right)\left[1-\left(\frac{r}{\lambda R}\right)^2\right] \tag{3}$$

and the volumetric flow rate q^I in region I, which is one-twelfth of the volumetric flow rate in the whole fiber, is obtained by the Hagen-Poiseuille law:

$$q^I = -\frac{dP^I}{dz}\left(\frac{\lambda^4R^4\pi}{96\mu}\right) \tag{4}$$

The velocity profile for the flow through the outside of the fiber, region II, is more complex than that in region I. In region II, the fluid velocity depends not only on the radial coordinate r but also on the angular coordinate θ because of the presence of the neighboring fibers. Sparrow and Loeffler (1959) obtained the solution for the velocity profile of a flow through an assemblage of uniformly packed cylindrical rods. Their solution which is directly applicable to the present flow geometry is given by

$$v^{II} = -\frac{dp^{II}}{dz}\left(\frac{R^2}{\mu}\right)\left\{\frac{\sqrt{3}\sigma^2}{\pi}\ln\frac{r}{R}+\frac{1}{4}\left[1-\left(\frac{r}{R}\right)^2\right] + \sum_{n=1}\gamma_n\left[\left(\frac{r}{R}\right)^{6n}-\left(\frac{R}{r}\right)^{6n}\right]\cos 6n\theta\right\} \tag{5}$$

The series constants γ_n are functions of the pitch-to-diameter ratio σ. Sparrow (1959), Axford (1967), and Dwyer (1970) have reported values for γ_n or for related parameters as functions of σ. The volumetric flow rate q^{II} can be expressed in terms of the dimensionless pressure drop-flow parameter ϕ:

$$q^{II} = -\frac{dP^{II}}{dz}\left(\frac{R^4}{\mu\phi}\right) = \int\int v^{II}\, r\, dr\, d\theta \tag{6}$$

By integrating the velocity v^{II} over the flow area in region II, we have the expression for the pressure drop-flow parameter ϕ as a function only of the pitch-to-diameter ratio σ.

It is assumed that the shape of the well-developed cross sectional concentration profile is constant throughout the major part of the dialyzer. Although this particular condition is not essential for solving the partial differential equations describing the mass transfer system (Gill and Nunge, 1966), it simplifies the mathematical treatment drastically. According to the constant profile assumption, the solute flux across the membrane is constant for any axial coordinate z, and the volumetric flow rates of the fluids in region I and region II are equal in magnitude but opposite in direction:

$$q^I + q^{II} = 0 \tag{7}$$

From Equations (4), (6), and (7), the pressure drops of the flows in region I and region II are related by

$$\frac{dP^{II}}{dz} = -\left(\frac{\pi\phi\lambda^4}{96}\right)\frac{dP^I}{dz} \tag{8}$$

Since the solute flux is invariant with the axial coordinate, the bulk concentrations $u_b{}^I$ and $u_b{}^{II}$ are linear functions of z. Furthermore, from the countercurrent equal volumetric flow condition, it can be shown that the axial bulk concentration gradients in regions I and II become identical to each other. The axial concentration gradients are related by

$$\frac{du^I}{dz} = \frac{du^{II}}{dz} = \text{constant} \tag{9}$$

From Equations (8) and (9), a characteristic concentration u^* for this system is defined:

$$\left(\frac{dP^I}{dz}\right)\left(\frac{du^I}{dz}\right)\left(\frac{\pi\lambda^4R^4}{96\mu\mathcal{D}}\right) = -\left(\frac{dp^{II}}{dz}\right)\left(\frac{du^{II}}{dz}\right)\left(\frac{R^4}{\phi\mu\mathcal{D}}\right) = u^* \tag{10}$$

Concentration Profiles

The cross-sectional concentration profiles of a countercurrent dialyzer can be described by a differential mass balance, or the equation of continuity. The equation of continuity which applies to our system is

$$\frac{\partial^2u}{\partial r^2}+\frac{1}{r}\frac{\partial u}{\partial r}+\frac{1}{r^2}\frac{\partial^2u}{\partial\theta^2}=\frac{1}{\mathcal{D}}\frac{\partial u}{\partial z}v \tag{11}$$

The axial diffusion term $\partial^2u/\partial z^2$ is usually much smaller than the other diffusion terms. In the present case, the concentration u is linear with the axial coordinate [Equation (9)], so that this term can be dropped. Solving Equation (11) for the velocity profiles developed in Equations (3) and (5) and for the stationary membrane, the cross-sectional concentration profile for each of the regions is obtained:

$$u^I/u^* = A^I + B^I\ln\frac{r}{R} + \sum_{k=1}\left[C_k{}^I\left(\frac{r}{\lambda R}\right)^k + D_k{}^I\left(\frac{\lambda R}{r}\right)^k\right]$$

$$[F_k^I \sin k\theta + E_k^I \cos k\theta]$$
$$-\frac{6}{\pi}\left(\frac{r}{\lambda R}\right)^2\left[1-\frac{1}{4}\left(\frac{r}{\lambda R}\right)^2\right] \quad (12)$$

$$u^M/Ku^* = A^M + B^M \ln\frac{r}{R} + \sum_{k=1}\left[C_k^M\left(\frac{r}{R}\right)^k + D_k^M\left(\frac{R}{r}\right)^k\right][F_k^M \sin k\theta + E_k^M \cos k\theta] \quad (13)$$

$$u^{II}/u^* = A^{II} + B^{II}\ln\frac{r}{R} + \sum_{k=1}\left[C_k^{II}\left(\frac{r}{R}\right)^k + D_k^{II}\left(\frac{R}{r}\right)^k\right][F_k^{II}\sin k\theta + E_k^{II}\cos k\theta] + \phi\left(\frac{r}{R}\right)^2\left\{\frac{\sqrt{3}\sigma^2}{4\pi}\left[\ln\frac{r}{R}-1\right] + \frac{1}{16}\left[1-\frac{1}{4}\left(\frac{r}{R}\right)^2\right] + \frac{1}{4}\sum_{n=1}\left[\frac{1}{6n+1}\left(\frac{r}{R}\right)^{6n} + \frac{1}{6m-1}\left(\frac{R}{r}\right)^{6n}\right]\gamma_n \cos 6n\theta\right\} \quad (14)$$

The following boundary conditions are used to solve the integration constants A, B, etc. At the center of a fiber, the concentration u^I becomes

$$u^I = u_o \quad \text{at} \quad r = 0 \quad (15)$$

where u_o is the center of the fiber concentration, the value of which must be finite. If the net flux of a solute from region I to region II has a positive value, u_o becomes the maximum concentration in the cross section. The next boundary conditions are given at the planes of symmetry in the unit cell (Figure 2). The steady state net flux of any solute across the symmetry planes which bound the unit cell must be zero. There are three such planes:

$$\frac{\partial u}{\partial \theta} = 0 \quad \text{at} \quad \theta = 0 \quad (16)$$

$$\frac{\partial u}{\partial \theta} = 0 \quad \text{at} \quad \theta = \pi/6 \quad (17)$$

$$\frac{\partial u}{\partial r\cos\theta} = 0 \quad \text{at} \quad r\cos\theta = \sigma R \quad (18)$$

The first two planes separate the basic unit cell from the neighboring cells on either side which share the same fiber. The last symmetry plane separates the unit cell from that of the other fiber. The final set of boundary conditions is given by the continuity of flux and chemical potential at the inner and outer interfaces of the membrane with the solution phase. These are:

$$\mathcal{D}^I\frac{\partial u^I}{\partial r} = \mathcal{D}^M\frac{\partial u^M}{\partial r} \quad \text{at} \quad r = \lambda R \quad (19)$$

$$\mathcal{D}^M\frac{\partial u^M}{\partial r} = \mathcal{D}^{II}\frac{\partial u^{II}}{\partial r} \quad \text{at} \quad r = R \quad (20)$$

and

$$u^M = K\,u^I \quad \text{at} \quad r = \lambda R \quad (21)$$

$$u^M = K\,u^{II} \quad \text{at} \quad r = R \quad (22)$$

Using the boundary conditions given in Equations (15) to (22), the expressions for all of the integration constants in Equations (12) to (14) are obtained. The concentration profiles are given in terms of series constants δ_n:

$$\frac{u_o - u^I}{u^*} = \frac{6}{\pi}\left(\frac{r}{\lambda R}\right)^2\left[1-\frac{1}{4}\left(\frac{r}{\lambda R}\right)^2\right] - \sum_{n=1}\left(\frac{r}{\lambda R}\right)^{6n}\delta_n \cos 6n\theta \quad (23)$$

$$\frac{u_o - u^M/K}{u^*} = \frac{6}{\pi}\left[\frac{3}{4}+\frac{1}{\xi}\ln\frac{r}{\lambda R}\right] - \frac{1}{2}\sum_{n=1}\left[\left(1+\frac{1}{\xi}\right)\left(\frac{r}{\lambda R}\right)^{6n} + \left(1-\frac{1}{\xi}\right)\left(\frac{\lambda R}{r}\right)^{6n}\right]\delta_n \cos 6n\theta \quad (24)$$

$$\frac{u_o - u^{II}}{u^*} = \frac{6}{\pi}\left[\frac{3}{4}+\left(1-\frac{1}{\xi}\right)\ln\lambda + \ln\frac{r}{\lambda R}\right] + \frac{\phi}{64}\left[3-4\left(\frac{r}{R}\right)^2+\left(\frac{r}{R}\right)^4+4\ln\frac{r}{R}\right] - \frac{\sqrt{3}\sigma^2\phi}{4\pi}\left[1-\left(\frac{r}{R}\right)^2+\ln\left(\frac{r}{R}\right)+\left(\frac{r}{R}\right)^2\ln\left(\frac{r}{R}\right)\right] - \frac{\phi}{4}\left(\frac{r}{R}\right)^2\sum_{n=1}\left[\frac{1}{(6n+1)}\left(\frac{r}{R}\right)^{6n} + \frac{1}{(6n-1)}\left(\frac{R}{r}\right)^{6n}\right]\gamma_n \cos 6n\theta + \frac{\phi}{4}\sum_{n=1}\left[\frac{1}{(6n-1)}\left(\frac{r}{R}\right)^{6n} + \frac{1}{(6n+1)}\left(\frac{R}{r}\right)^{6n}\right]\gamma_n \cos 6n\theta$$

$$-\frac{1}{4}\sum_{n=1}\left\{\begin{array}{l}\left[\left(1+\frac{1}{\xi}\right)(1+\xi)\lambda^{-6n}+\left(1-\frac{1}{\xi}\right)(1-\xi)\lambda^{6n}\right]\left(\frac{r}{R}\right)^{6n} \\ +\left[\left(1+\frac{1}{\xi}\right)(1-\xi)\lambda^{-6n}+\left(1-\frac{1}{\xi}\right)(1+\xi)\lambda^{6n}\right]\left(\frac{R}{r}\right)^{6n}\end{array}\right\}\delta_n \cos 6n\theta \quad (25)$$

The concentration profiles are defined in terms of the two infinite series: γ_n defined from the equation of motion in region II, previously evaluated, and δ_n which can be determined from the boundary condition given in Equation (18), using either the method of point matching (Sparrow and Loeffler, 1959; Dwyer, 1970) or the method of least-square fitting (Rakowsky and Epstein, 1968; France, 1971).

RESULTS

The right-hand side of Equations (23) to (25) can be evaluated explicitly as functions of r and θ if the values of σ, λ, and ξ are fixed. Even though the concentration of a solute depends on the axial coordinate z, a normalized quantity which is independent of z can be selected to

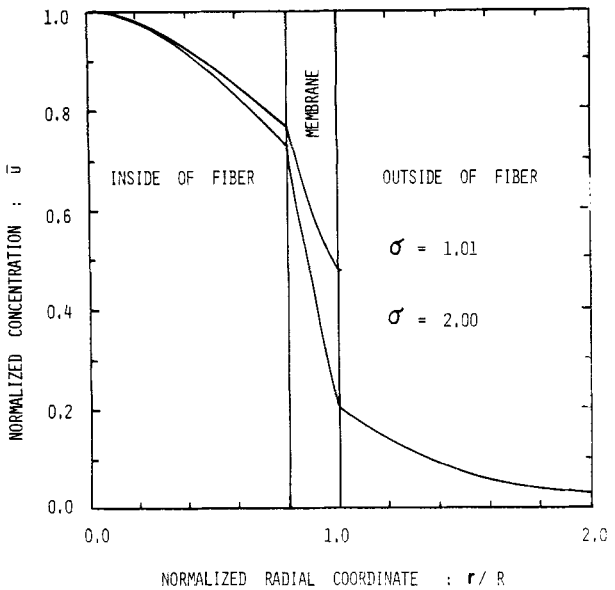

Fig. 3. Normalized solute concentration $\bar{u}$ as a function of normalized distance from the center of a fiber at $\Theta = 0$. ξ and λ are 0.15 and 0.8, respectively.

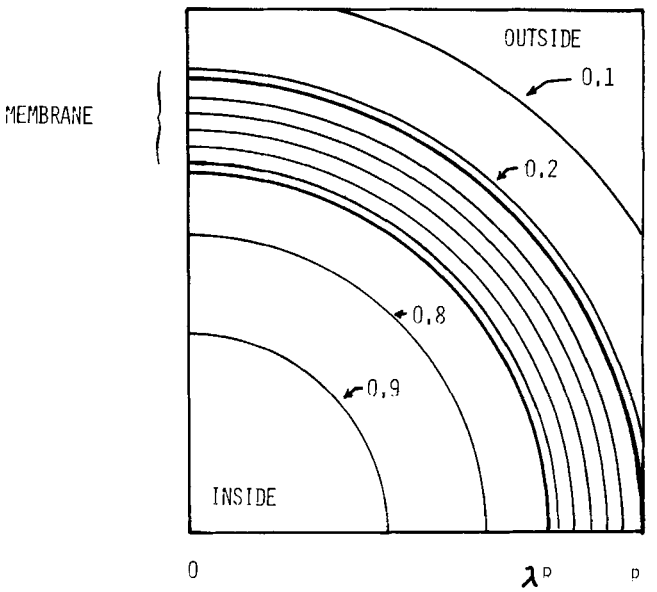

Fig. 4. Isotonic contours of normalized solute concentration in a widely spaced fiber array ($\sigma = 2$). ξ and λ are 0.15 and 0.8, respectively.

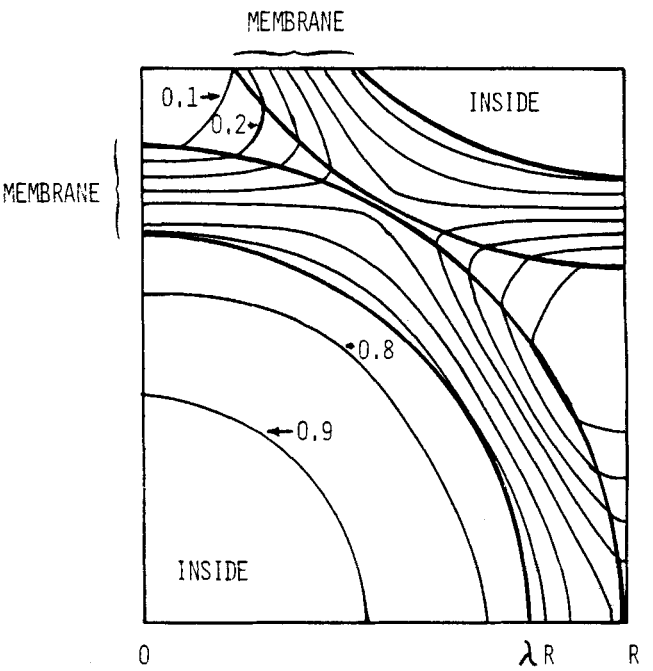

Fig. 5. Isotonic contours of normalized solute concentration in a closely spaced fiber array ($\sigma = 1.01$). ξ and λ are 0.15 and 0.8, respectively.

describe the cross-sectional concentration profile. The normalized cross-sectional concentration $\bar{u}$ is defined as

$$\bar{u} = \begin{cases} (u^I - u_c)/(u_o - u_c) & 0 \leq r < \lambda R \\ (u^M/K - u_c)/(u_o - u_c) & \text{if } \lambda R \leq r < R \\ (u^{II} - u_c)/(u_o - u_c) & R \leq r \leq \sigma R/\cos\theta \end{cases} \quad (26)$$

where u_c is the concentration of a solute at the point C of Figure 2. If the concentration of a solute inside a hollow fiber is higher than concentration outside, u_o and u_c become, respectively, the maximum and the minimum concentrations for a given cross section of the dialyzer.

Figure 3 is a typical cross-sectional concentration profile diagram. Normalized concentrations $\bar{u}$, for a tightly packed dialyzer ($\sigma = 1.01$) and for a relatively sparsely packed dialyzer ($\sigma = 2$), are plotted as functions of the dimensionless radial coordinate r/R at $\theta = 0$. The values for λ and ξ are 80 and 15% and are selected to approximate the actual dimensions of a Cuprophrane hollow fiber and the diffusivity data (Colton, 1971) for urea in similar membrane material. The concentration profile inside the fiber remains more or less the same for both pitch-to-diameter ratios. The concentration drop across the membrane, however, is greatly influenced by the packing density of the fibers. The tightly packed dialyzer shows only one half of the concentration drop, that is, the solute flux, compared to the transmembrane concentration drop for the dialyzer with loosely packed fibers.

Figures 4 and 5 show the isotonic contours in a quarter of a cross section of a hollow fiber. The magnitudes for the λ and ξ remain as 80 and 15%. The contours are drawn for an increment of one tenth in the normalized scale of $\bar{u}$. When the fibers are kept far apart from each other (Figure 4) and neighboring fibers have very little influence on the transport of solute, the isotonic contours have the shape of concentric circles. On the other hand, when the fibers are packed very tightly (Figure 5), there will be a definite interaction between neighboring fibers and the isotonic contours no longer have a circular shape.

Although the complete solution for the local concentration $\bar{u}$ has already been obtained in terms of r and θ, for practical purposes it is often desirable to develop a set of expressions to characterize the overall mass transfer behavior of the dialyzer. The average flux of a solute from one region to another is considered to be proportional to the difference in the characteristic phase concentrations representing the concentrations of the solute in each phase. In our system, these phase concentrations are the bulk concentrations of the fluids in regions I and II and the surface averaged wall concentrations at the inner and outer surfaces of the hollow fiber membrane. Since the local solute flow at any point in the basic unit cell is already available from Equations (23) to (25), analytical evaluation of the proportionality constants, that is, the mass transfer coefficients, is possible.

The average radial flux $J_{\lambda R}$ of a solute at the inner surface of the fiber is given by

$$J_{\lambda R} = (h^I/\lambda)(u_b{}^I - u_w{}^I) \quad (27)$$

where (h^I/λ) is the mass transfer coefficient assigned for the diffusional exchange of a solute between the bulk region I and the inner surface of the fiber. The surface averaged inner wall concentration $u_w{}^I$ and the bulk concentration $u_b{}^I$ in region I are evaluated from Equations (3), (4), and (23):

$$u_w{}^I = u_o - \frac{9}{2\pi} u \tag{28}$$

$$u_b{}^I = u_o - \frac{7}{4\pi} u^* \tag{29}$$

From a simple mass balance, the flux and the inner surface and the flux at the outer surface of the membrane are related by

$$J_R = \lambda J_{\lambda R} = h^I (u_b{}^I - u_w{}^I) \tag{30}$$

The average radial flux J_R at the outer surface can also be expressed in terms of different characteristic phase concentrations. If we use the form of Equation (27), similar expressions are obtained

$$J_R = h^M (u_w{}^I - u_w{}^{II}) \tag{31}$$

$$J_R = h^{II} (u_w{}^{II} - u_b{}^{II}) \tag{32}$$

where h^M and h^{II} are the mass transfer coefficients based on the outer surface of a fiber, the former one assigned for the transfer of a solute across the membrane and the latter for the transfer between the outer surface and the bulk in region II. The surface averaged outer wall concentration $u_w{}^{II}$ and the bulk concentration $u_b{}^{II}$ are evaluated from Equations (5), (6), and (25):

$$u_w{}^{II} = u_o - \left[\frac{9}{2\pi} - \frac{6}{\pi\xi}\ln\lambda\right] u^* \tag{33}$$

$$u_b{}^{II} = u_o - \psi u^* \tag{34}$$

The term ψ is a complicated function of σ, λ, and ξ:

$$\psi = \frac{1}{q^{II}} \int_0^{\pi/6} \int_R^{\sigma/R\cos\theta} \frac{u_o - u^{II}}{u^*} v^{II}\, r\, dr\, d\theta \tag{35}$$

The overall mass transfer coefficient h^o based on the outer surface is also defined:

$$J_R = h^o (u_b{}^I - u_b{}^{II}) \tag{36}$$

The surface averaged radial flux J_R of a solute at the outer surface of the fiber is evaluated directly from Equation (25):

$$J_R = \frac{6}{\pi} \frac{\mathcal{D}}{R} u^* \tag{37}$$

From Equations (30) to (32), (35), and (36), the mass transfer coefficients are obtained as functions of σ, λ, and ξ. They are normalized with the outer diameter $2R$ and the diffusivity $\mathcal{D}$ of the solute in a free solution to give a set of dimensionless moduli, or the Sherwood numbers:

$$Sh^I = \frac{2Rh^I}{\mathcal{D}} = \frac{48}{11} \tag{38}$$

$$Sh^M = \frac{2Rh^M}{\mathcal{D}} = \frac{2\xi}{\ln(1/\lambda)} \tag{39}$$

$$Sh^{II} = \frac{2Rh^{II}}{\mathcal{D}} = \frac{24\xi}{(2\pi\psi - 9)\xi - 12\ln\lambda} \tag{40}$$

$$Sh^o = \frac{48}{4\pi\psi - 7} \tag{41}$$

It is interesting to note that the Sherwood numbers and mass transfer coefficients which apply to the inside of the fiber and to the membrane are independent of the pitch-to-diameter ratio σ, so that these results must be valid for any value of σ. When hollow fibers are infinitely far apart from each other, the terms in Equations (23) to (25) which depend on the angular coordinate θ drop out. The results obtained in Equations (38) and (39) can, therefore, be applied to the situation in which there is no angular dependence of the concentration or the flux of a solute. When the concentration of a solute inside the fiber depends on r and z only, the problem is reduced to the extended Graetz problem (1885), the solution to which is well known for its application to heat transfer calculations. The asymptotic solution for the well-developed temperature field yields a Nusselt number of 48/11 (Sellars, 1956) which is in perfect agreement with Equation (38). The Sherwood number Sh^I is developed primarily for a system which shows a strong angular dependence on the concentration profile. Surprisingly, the Sherwood number within region I of the system is constant, regardless of the angular dependence of the concentration fields of the fiber. One can speculate that this result may, in fact, be independent of the packing geometry of the fiber bundle. The mass transfer coefficient h^M, both for the system with a θ dependent concentration profile and for the system of perfectly mixed solutions, can be expressed as

$$h^M = \frac{\mathcal{D}\xi}{R\ln(1/\lambda)} \tag{42}$$

From Equation (2), the numerator $\mathcal{D}\xi$ is the effective diffusivity of the solute in the membrane. When the membrane is relatively thin, so that the diameter ratio λ is near unity, the denominator $R\ln(1/\lambda)$ is approximately equal to the thickness of the membrane. The mass transfer coefficient h^M is often called the membrane permeability of the solute.

The Sherwood number Sh^{II} for the outside of the fiber is a function of the pitch-to-diameter ratio σ. Evaluation of this dimensionless number requires the numerical integration of Equation (35). Once the value for Sh^{II} is calculated, the overall Sherwood number Sh^o is obtained from Equation (36). Typical values for Sherwood numbers as functions of the diameter-to-pitch ratio $1/\sigma$ are plotted in Figure 6. The selected values for the inner-to-

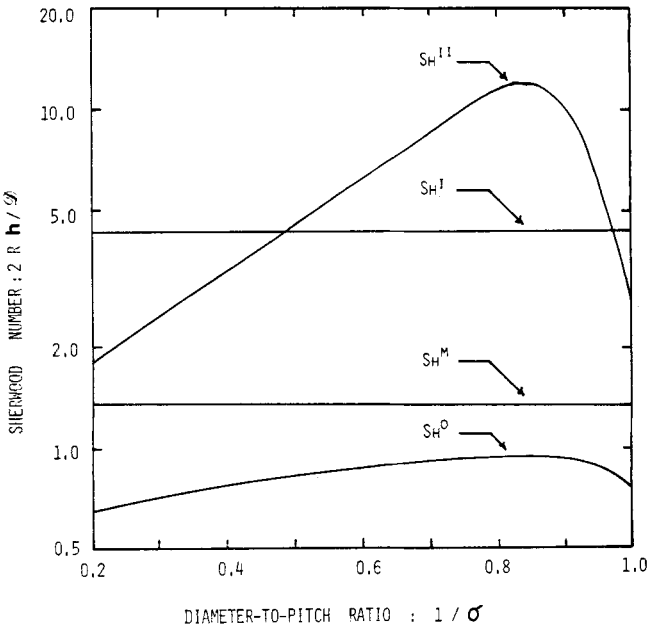

Fig. 6. Sherwood numbers Sh^o, Sh^I, Sh^M, and Sh^{II} as functions of $1/\sigma$. ξ and λ are 0.15 and 0.8, respectively.

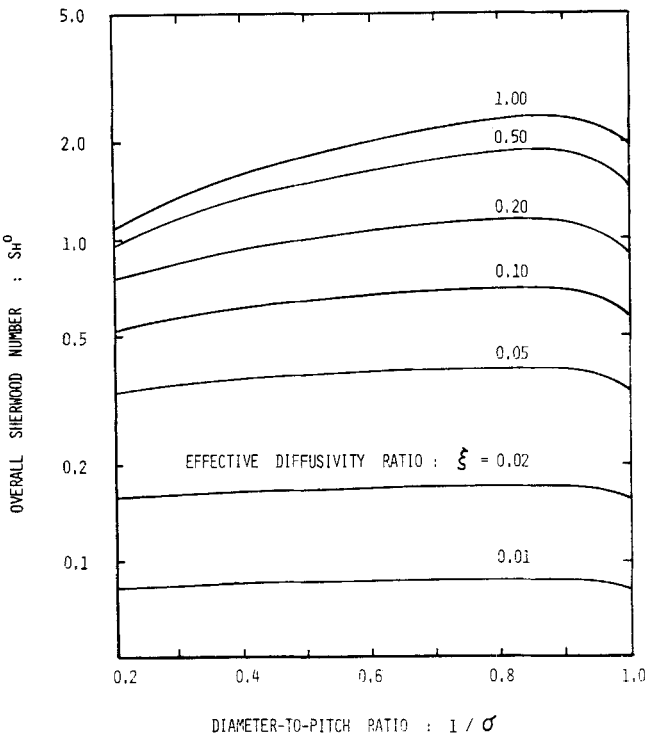

Fig. 7. Sh^0 vs. $1/\sigma$ for various ξ at $\lambda = 0.8$.

outer diameter ratio λ and the effective diffusivity ratio ξ are 80 and 15%. The most interesting feature of the plot is the shape of the curve for Sh^{II} which has a peak around $\sigma = 1.2$. A similar correlation curve having a maximum peak has been reported by Dwyer (1970) for the calculation of heat transfer coefficients in regularly packed nuclear fuel rod bundles. The result is explained in the following way. When the hollow fibers are kept sufficiently far apart, the average distance which the solute molecules must travel by diffusion from the bulk of region II to the outer surface of the membrane increases with the increase of the space between the fibers. The Sherwood number Sh^{II} decreases as the diameter-to-pitch ratio

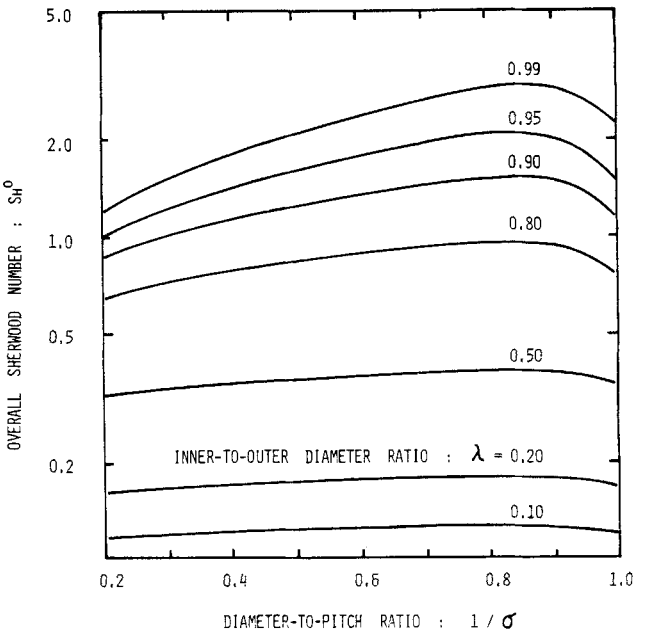

Fig. 8. Sh^0 vs. $1/\sigma$ for various λ at $\xi = 0.15$.

$1/\sigma$ decreases. On the other hand, when the fibers are packed very closely, that is, $1/\sigma$ is near unity, the flow of fluid is practically stagnant in the area where two fibers almost touch. The outer surface of the membrane is only partially exposed to the fluid flow in region II, so that the mass transfer coefficient h^{II} actually decreases with the increase of the diameter-to-pitch ratio $1/\sigma$. Thus, the shape of the curve for Sh^{II} in Figure 6 is thought to be the result of the combination of these two competing effects.

The effect of σ on the overall Sherwood number Sh^o is less pronounced than on Sh^{II}. The outside Sherwood number Sh^{II} shown in Figure 6 tends to be much larger than the membrane Sherwood number Sh^M for most of the practical ranges of σ; the contribution of Sh^{II} to Sh^o becomes relatively small. Thus, the overall Sherwood number is strongly influenced only by the inner-to-outer fiber

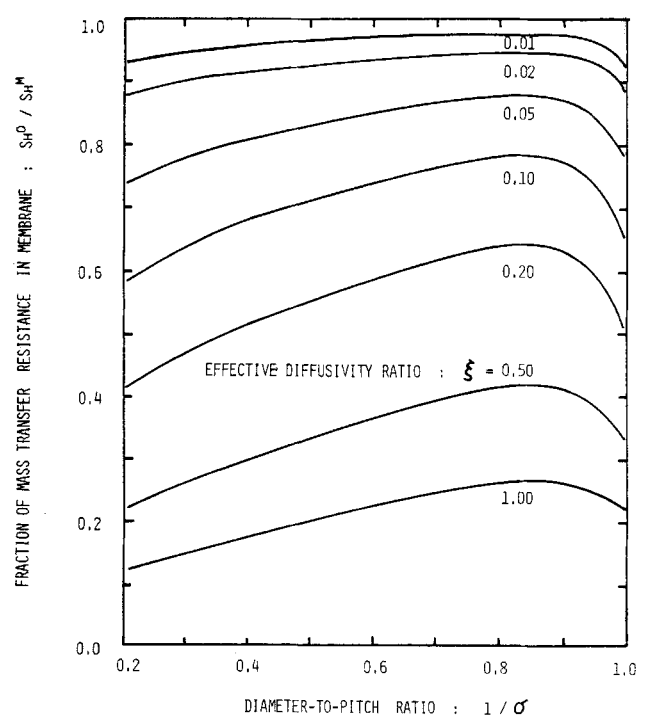

Fig. 9. Sh^0/Sh^M vs. $1/\sigma$ for various ξ at $\lambda = 0.8$.

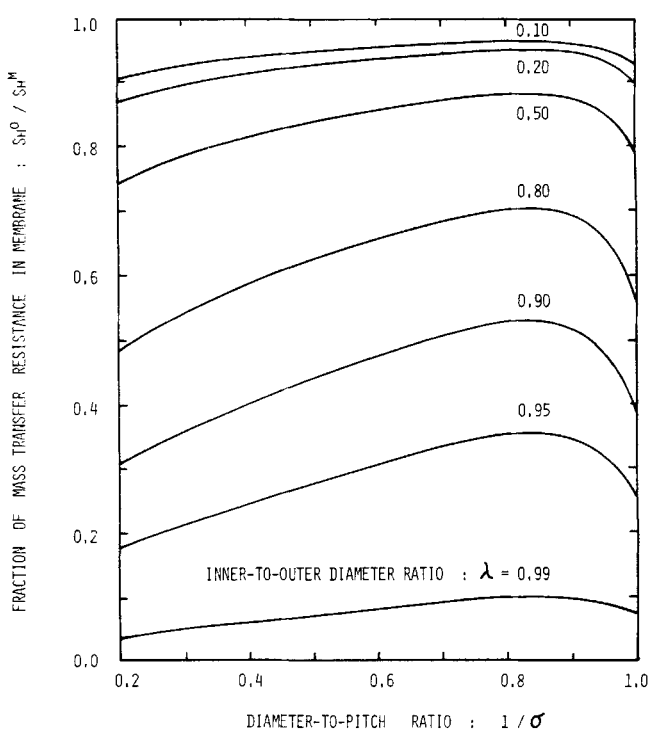

Fig. 10. Sh^0/Sh^M vs. $1/\sigma$ for various λ at $\xi = 0.15$.

diameter ratio λ and the effective diffusivity ratio ξ as shown in Figures 7 and 8. For highly permeable solutes and for very thin membranes, the peak shaped dependence of Sh^o on σ is evident. The effect is far less important when Sh^M is small, and the majority of the mass transfer resistance is provided by the membrane.

Figures 9 and 10 show the percent contribution of the membrane resistance for different values of λ and ξ. When the membrane is thin or highly permeable to the solute, the contribution of the membrane obviously is small, and this fact becomes very important when a dialyzer is used to separate two solutes by taking advantage of the difference in their permeability. The selectivity is defined as the ratio between effective diffusivities of the two solutes in a given phase. Since it becomes greater in the membrane than in free solution, any added contribution of the resistance from solution phase, either inside or outside the membrane, tends to decrease the overall selectivity of the dialyzer. Thus, even if the membrane selectivity is not a function of the thickness of the membrane, the overall selectivity of the dialyzer is often a function of the membrane thickness. Other parameters may be determined from Figures 9 and 10. By definition, the ratio between the Sherwood numbers is a ratio between mass transfer coefficients, so that the overall mass transfer coefficient is obtained by multiplication of the membrane permeability by the quantity Sh^o/Sh^M. The ratio Sh^o/Sh^M can be treated as a correction factor of the membrane permeability. For example, from Colton's data (1971), the membrane permeability and the value of ξ for urea in Cuprophrane are 6.1×10^{-2} cm/min and 0.15. Given Cuprophrane hollow fibers (0.03 cm OD and 0.028 cm ID), the expected overall mass transfer coefficient is calculated from Figure 10. The correction factors Sh^o/Sh^M for maximum packing density ($\sigma = 1$) and for optimal packing density ($\sigma = 1.2$) become 39 and 53%, respectively. The corresponding overall mass transfer coefficients are 2.4×10^{-2} and 3.3×10^{-2} cm/min. This large variation is caused only by a difference in the packing density of the fibers in the shell. A tightly packed dialyzer has a lower mass transfer coefficient in this case.

DISCUSSION

The physical condition required for this study is that of countercurrent equal volumetric flow. When the magnitude of the volumetric flow rates is different, the simplification [Equation (9)] used to solve the equation of continuity is no longer valid, and the solutions for the partial differential equations become extremely complicated. The aim of this study is to obtain a quantitative description of the effects of several important physical parameters on the mass transfer characteristics of a hollow fiber dialyzer. Thus, the general applicability of the result is sacrificed for mathematical simplicity.

The assumption of no volumetric flow across the membrane is introduced, again for mathematical simplicity. Unlike ultrafiltration and reverse osmosis hollow fiber units which have very high transmembrane pressure differences, the ordinary hollow fiber dialyzers have relatively small net volumetric flux of fluid through the membrane. By neglecting this additional flux of solution, a small error may be introduced into the calculated mass transfer coefficients.

The entry region effect in mass transfer is usually very important. The hollow fiber system is an exception because of the extremely large length-to-diameter ratio. The assumption of well-developed concentration profiles tends to underestimate the actual values of the mass transfer coefficients.

The most important and also the most unrealistic assumption is that of uniform fiber distribution. In a real dialyzer, the hollow fibers are packed randomly, and there is no regular array of triangular pitch configuration. Channeling of the fluid through the maldistributed hollow fibers is often experienced in a real system. This maldistribution decreases not only the mass transfer efficiency but also the selectivity of the dialyzer. These results obtained for a uniformly distributed array of hollow fibers should be treated as an upper limit of the physically achievable separation efficiency for a given hollow fiber dialyzer.

ACKNOWLEDGMENT

This research is taken from a thesis submitted by Isao Noda in partial fulfillment for the degree of Doctor of Philosophy in Chemical Engineering at Columbia University, 1978.

NOTATION

$A, B, \ldots H$ = integration constants
J = radial flux of solute (=) mole/s-cm^3
K = equilibrium partition coefficient of solute
P = pressure (=) dyne/cm^2
q = volumetric flow rate (=) cm^3/s
r = radial coordinate (=) cm
R = outer radius of a fiber (=) cm
Sh = Sherwood number
u = concentration = (mole/cm^3
u^* = characteristic concentration defined in Equation (10), (=) moles/cm^3
$\overline{u}$ = normalized cross-sectional concentration
v = velocity of fluid (=) cm/s
z = axial coordinate (=) cm

Italic Letters

$\mathcal{D}$ = diffusivity (=) cm^2/s

Greek Letters

γ_n = integration constants in infinite series
δ_n = integration constants in infinite series
θ = angular coordinate
λ = inner-to-outer diameter ratio of a fiber
μ = fluid viscosity (=) poise
ξ = effective diffusivity ratio
σ = pitch-to-diameter ratio
ϕ = pressure drop-flow parameter
ψ = function of σ, λ, and ξ defined in Equation (35)

Superscripts

I = inside of fiber
II = outside of fiber
M = in membrane
o = overall

Subscripts

b = bulk
w = wall

LITERATURE CITED

Axford, R. A., "Two-Dimensional Multiregion Analysis of Temperature Fields in Reactor Tube Bundles," *Nucl. Eng. Design*, 6, 25-42 (1967).

Colton, C. K., K. A. Smith, E. W. Merrill, and P. C. Farrell, "Permeability Studies with Cellulosic Membranes," *J. Biomed. Mater. Res.*, 5, 459-88 (1971).

Doshi, M. R., W. N. Gill, and V. N. Kabadi, "Optimal Design of Hollow Fiber Modules," *AIChE J.*, 23, 765 (1977).

Drew, T. B., "Mathematical Attacks on Forced Convection Problems," *Trans. Am. Inst. Chem. Engrs.*, 26, 76-80 (1931).

Dwyer, O. E., and H. C. Berry, "Laminar-Flow Heat Transfer for In-Line Flow Through Unbaffled Rod Bundles," *Nucl. Sci. Eng.*, **42**, 81-88 (1970).
Emersleben, O., "Das Darcysche Filtergesetz," *Physikalische Zeitschrift*, **26**, 601-10 (1925).
France, D. M., "Analytical Solution to Steady-State Heat-Conduction Problems," *J. Heat Transfer, Trans. ASME*, **93**, 449-454 (1971).
Frankel, D. S., and J. Wei, "Three Dimensional Tissue Culture With Forced Percolation," paper presented at 70th Annual Meeting, AIChE, New York (Nov., 1977).
Gill, W. N., and R. J. Nunge, "An Analytical Study of Laminar Counter Flow Double Pipe Heat Exchanger," *AIChE J.*, **12**, 279-289 (1966).
Gill, W. N., and B. Bansal, "Hollow Fiber Reverse Osmosis Systems Analysis and Design," *ibid.*, **19**, 823-831 (1973).
Graetz, L., "Ueber die Warmeleitungsfahigkeit von Flussigkeiten," *Ann. Physik*, **25**, 337-357 (1885).
Happel, J., "Viscous Flow Relative to Arrays of Cylinders," *AIChE J.*, **5**, 174-177 (1959).
Kim, S. S., and D. O. Cooney, "Improved Theory for Hollow Fiber Enzyme Reactors," *Chem. Eng. Sci.*, **31**, 289-294 (1976).
Klein, E., E. F. Holland, A. Lebeouf, A. Donnaud, and J. K. Smith, "Transport and Mechanical Properties of Hemodialysis Hollow Fibers," *J. Membrane Sci.*, **1**, 4 (1976*a*).
Klein, E., and F. Holland, in "Membrane and Materials Evaluation," Proc. 9th Annual Contractors' Conference, p. 74, (NIH-77-1167), AK-CUP, NIAMDD, NIH, Bethesda, Md. (1976*b*).
———, et al., "Evaluation of Hemodialyzers and Dialysis Membranes," *Publ. No. NIH-77-1294*, U.S. Dept. HEW (1977).
Krough, A., "Number and Distribution of Capillaries in Muscles with Calculations of the Oxygen Pressure Head Necessary for Supplying the Tissue," *J. Physiol.*, **52**, 409-415 (1918).
Leonard, E. F., and T. G. Kaufman, "Mechanism of Interfacial Mass Transfer in Membrane Transport," *AIChE J.*, **14**, 110-119 (1968).
Lih, M. M., *Transport Phenomena in Medicine and Biology*, Wiley, New York (1975).
Michaels, A. S., "Analysis of Membrane Transport Devices," *Trans. Am. Soc. Artif. Int. Organs*, **12**, 387-392 (1966).
Mottaghian, R., and L. Wolf, "Fully Developed Laminar Flow in Finite Rod Bundles of Arbitrary Arrangement," *Trans. Am. Nucl. Soc.*, **15**, 876-885 (1972).
Noda, I, S. Sea, and C. C. Gryte, "Selective Separation by Coupled Cascaded Dialysis and Ultrafiltration," paper presented at AIChE Meeting, Chicago, Ill. (Dec., 1976).
Presser, K. H., "Mass Transfer and Pressure Losses in Parallel Flow Through Rod Clusters Within a Wide Range of Reynolds Numbers and Pitches," *Int. J. Heat Mass Transfer*, **14**, 1235-1259 (1971).
Rakowsky, D. A., and N. Epstein, "Laminar Flow in Regular Polygonal Shaped Ducts with Circular Centered Cores," *Can. J. Chem. Engr.*, **46**, 22-26 (1968).
Rehme, K., "Pressure Drop Performance of Rod Bundles in Hexagonal Arrangements," *Int. J. Heat Mass Transfer*, **15**, 2499-2517 (1972).
Schmid, J., "Longitudinal Laminar Flow in an Array of Circular Cylinders," *Int. J. Heat Mass Transfer*, **9**, 925-937 (1966).
Sellars, J. R., M. Tribus, and J. S. Klein, "Heat Transfer to Laminar Flow in a Round Tube or Flat Conduit," *Trans. ASME*, **78**, 441-448 (1956).
Shih, F. S., "Laminar Flow in Axisymmetric Conduits by a Rational Approach," *Can. J. Chem. Eng.*, **45**, 285-294 (1967).
Sparrow, E. M., and L. A. Loeffler, "Longitudinal Laminar Flow Between Cylinders Arranged in Regular Arrays," *AIChE J.*, **5**, 325-330 (1959).
———, and H. A. Hubbard, "Heat Transfer to Longitudinal Laminar Flow Between Cylinders," *J. Heat Trans., Trans. ASME, Ser. C*, **83**, 415-422 (1961).
Stevenson, J. F., M. A. Van Deak, M. Weinberg, and R. W. Schuette, "Unsteady State Method for Measuring Permeability of Small Tubular Reactors," *AIChE J.*, **21**, No. 6, 1192-1199 (1975).
Sullivan, R. R., "Specific Surface Measurements on Compact Bundles of Parallel Fibers," *J. Appl. Phys.*, **13**, 725-730 (1942).
Waterland, L. R., A. S. Michaels, and C. R. Robertson, "Theoretical Model for Enzymatic Catalysis Using Asymmetric Hollow Fiber," *AIChE J.*, **20**, 50-59 (1974).
Winograd, Y., M. Toren, and A. Solan, "Mass Transfer in Counter-Flow Shell and Tube Mass Exchangers," *Israel J. Tech.*, **9**, 381-387 (1971).
———, "Reverse Osmosis in Shell and Tubes," *Desalination*, **14**, No. 2, 173-187 (1974).

Manuscript received November 22, 1977; revision received August 11 and accepted August 25, 1978.

Gas Absorption by a Liquid Layer Flowing on the Wall of a Pipe

WILLIAM H. HENSTOCK
and
THOMAS J. HANRATTY
University of Illinois
Urbana, Illinois 61801

A method is presented for predicting absorption rates for liquid layers flowing along a wall. It is based on results presently available in the literature as well as on the results of studies we recently carried out on the rate of oxygen absorption from a flowing air stream into water layers on the bottom of a horizontal enclosed channel and on the inside of a vertical pipe. Absorption measurements can be interpreted by assuming that the process is controlled by eddies whose length and velocity are characterized by bulk turbulence properties and that in a region of thickness δ close to the interface the turbulence is dampened by viscosity.

SCOPE

The absorption of a gas by a flowing liquid film, for which the primary resistance to mass transfer is in the liquid phases, is an important commercial process. Kamei and Oishi (1955), Lamourelle and Sandall (1972), Emmert and Pigford (1954), Menez and Sandall (1974), Stirba and Hurt (1955), Coeuret et al. (1970), Miller (1949), and Vyazovov (1940) have measured rates of ab-

Correspondence concerning this paper should be addressed to Thomas J. Hanratty.